JB
Journals.ASM.org

Conjugal Transfer of Polychlorinated Biphenyl/Biphenyl Degradation Genes in *Acidovorax* sp. Strain KKS102, Which Are Located on an Integrative and Conjugative Element

Yoshiyuki Ohtsubo, Yoko Ishibashi, Hideaki Naganawa, Satoshi Hirokawa, Satomi Atobe, Yuji Nagata, and Masataka Tsuda

Department of Environmental Life Sciences, Graduate School of Life Sciences, Tohoku University, Katahira, Sendai, Japan

A polychlorinated biphenyl (PCB)/biphenyl degradation gene cluster in *Acidovorax* sp. strain KKS102, which is very similar to that in Tn*4371* from *Cupriavidus oxalaticus* A5, was transferred to several proteobacterial strains by conjugation. The mobilized DNA fragment consisted of 61,807 bp and carried genes for mating-pair formation (*mpf*), DNA transfer (*dtr*), integrase (*int*), and replication-partition proteins (*rep-parAB*). In the transconjugants, transferred DNA was integrated at ATTGCATCAG or similar sequences. The circular-form integrative and conjugative element (ICE) was detected by PCR, and quantitative PCR analyses revealed that, in KKS102 cells, the ratio of the circular form to the integrated form was very low (approximately 10^{-5}). The circular form was not detected in a mutant of the *int* gene, which was located at the extreme left and transcribed in the inward direction, and the level of *int* transcriptional activity was much higher in the circular form than in the integrated form. These findings clearly demonstrated that the genes for PCB/biphenyl degradation in KKS102 cells are located on an ICE, which was named ICE_{KKS102}*4677*. Comparisons of similar ICE-like elements collected from the public database suggested that those of beta- and gammaproteobacteria were distinguishable from other ICE-like elements, including those in alphaproteobacteria, with respect to the gene composition and gene organization.

Bacterial horizontal gene transfer plays an important role in the acquisition of new phenotypic traits and helps host cells adapt to their environments. Mobile genetic elements that carry genes for xenobiotic-compound degradation are of particular interest, because such elements contribute to the spread of genetic information that enables the host cell to degrade man-made chemicals.

Among the several classes of mobile genetic elements are integrative and conjugative elements (ICEs) (2, 3, 35) that, by being excised from genomes, form plasmid-like circular structures, transfer to other cells by conjugation, and reintegrate into the genomes of new hosts. The excision of ICEs from the genome involves the activity of integrase, which excises the circular entity from the genome by recombining the DNA tract found at each end of the ICE. The integrase also catalyzes the integration of the circular form into the genome. In the integration process, the integrase mediates recombination between the *attP* site on the circular-form DNA and the *attB* site on the genome of the recipient cell.

ICEs are known to encode a variety of phenotypic traits, including pathogenicity, resistance to antibiotics, and xenobiotic degradation (35). Examples of ICE-carrying genes for the degradation of xenobiotic compounds are limited to the *clc* element (105 kb) from *Pseudomonas knackmussii* B13 (23) and the *bph-sal* element (90 kb) from *Pseudomonas putida* KF715 (17); these elements carry degradation genes for 3-chlorobenzoate and polychlorinated biphenyl (PCB)/biphenyl plus salicylate, respectively. *Acidovorax* sp. strain KKS102, which is a betaproteobacterium, carries a *bph* operon for the conversion of PCB/biphenyl to the tricarboxylic acid (TCA) cycle intermediates. All of the genes necessary for the conversion are located in the *bph* operon (6, 8–10). The transcription of the *bph* operon depends on a single promoter, named pE, which responds to a metabolite of biphenyl (19) (substrate induction), as well as to the presence of favorable organic compounds (30) (catabolite control). Substrate induction and catabolite control are mediated by BphS, a transcriptional repressor, and a two-component regulatory system, BphPQ, respectively. The *bphS* gene is located proximal to the *bph* operon, whereas the *bphPQ* genes are distant from the *bph* operon.

A very similar *bph* operon was identified in *Cupriavidus oxalaticus* A5 (formerly *Ralstonia* sp. strain A5) by Toussaint et al., and the operon was shown to be part of a 54.7-kb transposon, Tn*4371* (32). In the same study, the complete nucleotide sequence of Tn*4371*, as well as seven related elements, was reported (32). Since then, a number of related elements have been reported. Van Houdt et al. described two similar elements residing in the genome of *Cupiriavidus metallidurans* CH34 (33). Ryan et al. described 18 related elements from beta- and gammaproteobacteria (27) and presented a list of genes conserved among the Tn*4371*-like elements in beta- and gammaproteobacteria. A recent study also added several other elements and described the conserved genes and their predicted functions (34). The last two studies referred to the collection of Tn*4371*-like elements as the Tn*4371* family of ICEs. However, none of the elements have so far been proven to transfer conjugally. Although Tn*4371* has been considered an ICE on the basis of its gene contents and the detection of covalently linked Tn*4371* ends, intercellular transfer of Tn*4371* has not yet been observed, and only the intracellular transposition of Tn*4371* has been proven (12, 27, 32). The right part of Tn*4371*, called Tn-*bph*, is capable of horizontal transfer, a process thought

Received 5 March 2012 **Accepted** 25 May 2012
Published ahead of print 8 June 2012
Address correspondence to Yoshiyuki Ohtsubo, yohtsubo@ige.tohoku.ac.jp.
Supplemental material for this article may be found at http://jb.asm.org/.

doi:10.1128/JB.00352-12

TABLE 1 Bacterial strains and plasmids used in this study

Strain or plasmid	Relevant characteristics	Source or reference
Strains		
E. coli		
DH5α	λ⁻ ϕ80d*lacZ*ΔM15 Δ(*lacZYA-argF*)*U169 recA1 endA1 hsdR17*(r_K^- m_K^-) *supE44 thi-1 gyrA relA1*	28
Acidovorax sp.		
KKS102	PCB/biphenyl degrader	10
KKS-SA4	KKS102 derivative carring Tc^r gene in the 22-nucleotide downstream region of the *bphS* gene, constructed by using linearized pSA4	This study
KKS-SA7	KKS-SA4 derivative, in which *traR* gene was replaced by Cm^r gene, constructed by using linearized pSA7	This study
KKS-SA10	KKS102 derivative, in which the *bphS* gene was replaced by the Tc^r gene, constructed by using linearized pSA10	This study
SA4GZintI	KKS-SA4 derivative carrying a single copy of the reporter construct on pGZintI in the genome	This study
SA4GZintC	KKS-SA4 derivative carrying a single copy of the reporter construct on pGZintC in the genome	This study
SA7GZintI	KKS-SA7 derivative carrying a single copy of the reporter construct on pGZintI in the genome	This study
SA7GZintC	KKS-SA7 derivative carrying a single copy of the reporter construct on pGZintC in the genome	This study
SA10GZintI	KKS-SA10 derivative carrying a single copy of the reporter construct on pGZintI in the genome	This study
SA10GZintC	KKS-SA10 derivative carrying a single copy of the reporter construct on pGZintC in the genome	This study
KKS-SA4Δint	KKS-SA4 derivative, in which the *int* gene was replaced by the kanamycin resistance gene	This study
B. multivorans		
ATCC 17616	Soil isolate	31
BmGm	Gm^r derivative of ATCC 17616, obtained by transforming ATCC 17616 with pTn*Mod*-OGm	This study
BmKm	Km^r derivative of ATCC 17616	This study
BmGmSA33	Transconjugant obtained by mating of BmGm and SA10; ICE is integrated at positions 1343869–1343870 in chromosome I	This study
BmGmSA35	Transconjugant obtained by mating of BmGm and SA10; ICE is integrated at positions 977691–977699 in chromosome I	This study
BmGmSA101, BmGmSA103	Transconjugant obtained by mating of BmGm and SA10; ICE is integrated at positions 2631253–2631244 in chromosome I	This study
BmGmSA102	Transconjugant obtained by mating of BmGm and SA10; ICE is integrated at positions 3445086–3445094 in chromosome I	This study
BmKmSA36	Transconjugant obtained by mating of BmKm and SA10; ICE is integrated at positions 434184–434192 in chromosome III	This study
S. japonicum		
Sp-UT26	HCH degrader	15
Sp-UTKm	Km^r derivative of UT26; *linA* mutant	Laboratory collection
UTKmSA11, UTKmSA14, UTKmSA15, UTKmSA121, UTKmSA122	Transconjugants obtained by mating of UTKm and KKS-SA10; ICE is integrated at positions 2157304–2157312 in chromosome I	This study
P. putida		
KT2440	Type strain; ATCC 47054; Cm^r	16
Pp-KTGm (KT2440G)	KT2440::Tn*Mod*-OGm; Gm^r	14
Pp-TKT1	Transconjugant obtained by mating of KTGm and KKS-SA4; ICE is integrated at positions 4361712–4361720	This study
Pp-TKT101	Transconjugant obtained by mating of KTGm and KKS-SA4; integration site not known	This study
KTGmSA151	Transconjugant obtained by mating of KTGm and KKS-SA10; ICE is integrated at positions 4361712–4361720	This study
PpY512	Km^r derivative of *P. putida* PpY101 carrying pE promoter fused with *lacZ*	30
Plasmids		
pKS13	RP4-based cosmid vector; Tet^r	10
pKH1	pKS13 derivative; carries entire *bph* genes	10
pKH3000	pKS13 derivative; carries downstream region of *bph* genes	This study
pKH5000	pKS13 derivative; carries upstream region of *bph* genes	This study
pKLZ-X	A plasmid for integration of promoter-*lacZ* fusion construct into genome of KKS102	30
pKLZG	pKLZ-X derivative; carries *gfp* gene from pGreenTIR in front of the *lacZ* gene	This study
pGZintC	pKLZG derivative; carries *int* upstream region (in its circular form) in front of the *gfp* gene	This study
pGZintI	pKLZG derivative; carries the *int* upstream region (in its integrated form) in front of the *gfp* gene	This study
pNIT6012	Tet^r; broad-host-range cloning vector	Accession no. AB043476
pNITGm	pNIT6012 derivative; Gm^r	Laboratory collection
pReInt2	pNITGm derivative; inserted in *int* gene in the multicloning site	This study
pTnMod-OGm	mini-Tn*5* transposon carrying the Gm^r gene	5
pHSG399	Cm^r	Accession no. M19087
pUC19	pMB9 replicon; Ap^r	36
pSA4	pHSG399 derivative; Tc^r gene integration plasmid in 22-nucleotide downstream region of *bphS*	This study
pSA7	pUC19 derivative; constructed to replace the *traR* with the Cm^r gene	This study
pSA10	pHSG399 derivative; constructed to replace *bphS* with the Tc^r gene	This study

to rely on the host genes, and furthermore, the boundaries of the transferred entity have been only roughly characterized by Southern blot analysis (12, 32). In addition, although related elements have also been found, mainly from alphaproteobacteria, whether they should be included in the same family of ICEs has not been addressed.

The high level of sequence similarity between the Tn*4371 bph* locus and the known DNA sequence of the KKS *bph* locus suggested that the *bph* locus of KKS102 might be a part of the mobile genetic element. In this study, we found that the *bph* operon from KKS102 was located on an ICE and that this ICE conjugally transferred to several strains belonging to different proteobacterial classes. We also collected a diversity of similar ICEs, including those from alphaproteobacteria, and concluded that ICE-like elements of beta-and gammaproteobacteria could be distinguished from those of alphaproteobacteria based on the gene content and gene order.

MATERIALS AND METHODS

Bacterial strains, plasmids, and culture conditions. The bacterial strains and plasmids used in this study are listed in Table 1. *Escherichia coli* strains were grown at 37°C in Luria-Bertani (LB) broth, and other bacterial cells

were grown at 30°C in 1/3 LB broth (0.33% tryptone, 0.16% yeast extract, and 0.5% NaCl). Cells carrying plasmids were incubated in the presence of antibiotics at concentrations of 50 mg/liter for ampicillin (Ap), 50 mg/liter for kanamycin (Km), 10 mg/liter for gentamicin (Gm), 50 mg/liter for tetracyclin (Tc), and 100 mg/liter for chloramphenicol (Cm). When required, 5-bromo-4-chloro-3-indolyl-β-D-galactopyranoside (X-Gal) was added to the media at a final concentration of 40 mg/liter. The cosmid library, from which two cosmid clones carrying *bph* upstream and downstream regions were obtained, was constructed in our previous study (30). To test whether transconjugants could grow on biphenyl, M9 minimal medium was used, and biphenyl was supplied as vapor from crystals placed on the lid of an inverted plate.

Primers. The primers used in this study are listed in Table S1 in the supplemental material.

Construction of strains. The derivatives of KKS102 (Table 1) were constructed by replacing part of the ICE region with an antibiotic resistance gene by two rounds of allelic exchange. For each derivative, a plasmid carrying an antibiotic resistance gene, flanked by two DNA regions for allelic exchanges, was constructed. Each plasmid was linearized by restriction enzyme digestion within the vector sequence and introduced into KKS102 cells by electroporation. To confirm whether an antibiotic resistance gene was inserted into the expected genomic site, the resulting antibiotic-resistant clones were investigated by PCR. For each PCR, a set of two primers was used, one annealing to the antibiotic resistance gene and the other to a region external to the cloned DNA region. This primer set gives a PCR product with reasonable length only when the expected homologous-recombination events have taken place. The Tc, Cm, and Km resistance genes were from pBR322, pHSG399, and pUC4K, respectively. pSA4 is a plasmid for insertion of the Tc resistance gene into a downstream region of *bphS*. pSA4 carries a DNA region spanning nucleotide positions 27139 to 27635 (relative to the left end of ICE$_{KKS102}$*4677*), the Tc resistance gene, and a DNA region spanning positions 27639 to 28058. pSA10 is a plasmid for the replacement of the *bphS* gene with the Tc resistance gene. pSA10 carries a DNA region spanning positions 27139 to 27635, the Tc resistance gene, and a DNA region spanning positions 29436 to 28587. pSA7 is for the replacement of the *bphR* gene with the Cm resistance gene. pSA7 carries a DNA region spanning positions 39443 to 41016, the Cm resistance gene, and a DNA region spanning from 42111 to 43039. pDint is a plasmid for replacement of the *int* gene with the Km resistance gene. pDint carries a DNA region spanning positions −510 to 299, the Km resistance gene, and a DNA region spanning from 1239 to 2047.

KKS-SA4 and KKS-SA10 were constructed by transforming KKS102 with linearized pSA4 and pSA10, respectively. KKS-SA7 was constructed by transforming KKS-SA4 with linearized pSA7. KKS-SA17 was constructed by transforming KKS-SA10 with linearized pSA7. The *int* mutant was constructed by transforming KKS-SA4 with linearized pDint. To supply the *int* mutant with the intact *int* gene in *trans*, plasmid pReInt2 was constructed. pReInt2 is a derivative of pNITGm and carries a DNA region spanning from 50 to 1453 that covers the *int* gene.

The *gfp-lacZ* reporter strains were constructed by using pKLZG, which is a derivative of pKLZ-X (19) and carries the *gfp* gene from pGreenTIR (13) in front of the *lacZ* gene. Each promoter DNA was ligated in front of the *gfp* gene, and the resulting plasmid, after linearization by restriction enzyme digestion, was used to transform KKS102 or its derivatives (see reference 19 for details). Two rounds of allelic exchange allowed stable integration of the reporter construct into a selected genomic region that is not close to ICE$_{KKS102}$*4677*. The following primers were used to amplify the promoter regions (see Fig. 4): for the construction of pGZintC (for the analysis of circular-form promoter activity), right-end_Eco and int_up_XbaI, and for the construction of pGZintI (for the analysis of integrated-form promoter activity), int_dis_A_EcoRI and int_up_XbaI.

BmGm and BmKm were constructed by transforming *Burkholderia multivorans* ATCC 17616 with pTn*Mod*-OGm and pTn*Mod*-OKm (5), respectively.

Mating experiment. Donor and recipient cells were grown to the end of the exponential growth phase in 2 ml of medium for about 12 h. Cells in the 2-ml cultures were mixed, centrifuged, and resuspended in 300 μl of fresh medium, and 50 μl of the suspension was spotted on membrane filters placed on solid medium without antibiotics. After incubation at 30°C from overnight to 4 days, the cells on the filter were suspended in fresh medium and plated on solid media containing appropriate antibiotics. When the transfer frequencies were very low, donor and recipient cells from 5-ml cultures were mixed and spotted onto fresh solid 1/3 LB medium for 4 days before plating on the selection medium. In mating experiments using KKS-SA4 (donor) and Pp-KTGm (recipient), transconjugants were selected on a plate containing Tc (50 mg/liter) and Gm (10 mg/liter). In addition, in mating experiments using KKS-SA4 (donor) and Sp-UTKm (recipient), transconjugants were selected on Tc (50 mg/liter) and Km (50 mg/liter), and in experiments using KKS-SA4 (donor) and BmGm (recipient), they were selected on Tc (50 mg/liter) and Gm (10 mg/liter). To exclude spontaneous drug-resistant clones, the colonies that appeared were tested for BphC activity. BphC activity was tested by adding a drop of 5% ethanol solution of the BphC substrate, 2,3-dihydroxybiphenyl, onto the colonies and then incubating the plates at room temperature for several minutes until the BphC-positive clones turned yellow. For the mating experiment with BmKmSA36 and Pp-KTGm, cells in midexponential phase were used. After mating on 1/3 LB medium for 15 h, cells were selected on solid medium containing Gm (10 mg/liter), Tc (30 mg/liter), and Cm (100 mg/liter). The colonies that appeared were tested for BphC activity, as well as for the emission of fluorescence under UV light, to discriminate colonies derived from BmKmSA36 and Pp-KTGm (Pp-KTGm, but not BmKmSA36, emits fluorescence under UV light).

Quantitative PCR. Quantitative PCR was conducted using a DNA engine option 2 thermal cycler (Bio-Rad Laboratories, Hercules, CA) and Cybr premix Ex Taq II (TaKaRa Bio, Shiga, Japan). The primers used to detect the circular form were primer 1 and primer 2, and those used to detect both forms were primer 3 and primer 4. The conditions for PCR were as follows: an initial cycle of 96°C for 3 min, followed by 30 cycles of 96°C for 15 s, 60°C for 15 s, and 72°C for 15 s and a final cycle of 72°C for 2 min. In a single run, one sample was measured at least in triplicate. For quantification, dilutions of PCR-amplified DNA fragments were used as standards.

DNA sequencing. To determine the DNA sequences of plasmids or PCR products, a BigDye thermal-sequencing kit version 1 and an ABI 310 genetic analyzer were used under the standard protocol. To directly obtain DNA sequence data from genomic DNA, a previously described method was used (18). In brief, 65 cycles of reactions were conducted in a 20-μl reaction mixture, which contained 4 μl of enzyme solution from a BigDye thermal-sequencing kit, 4 μl of 5× sequencing buffer (ABI), 3.3 pmol of primer, and 1 to 2 μg of genomic DNA. In the setting of running conditions for the 310 Genetic Analyzer, the injection time was extended from 30 s to 120 s. This change did not greatly affect the peak resolution of the electrophotogram in the ranges needed to determine the insertion site. On average, we determined a DNA sequence of 200 to 300 bases. Two primers, 3000_check_X3 and TKT-F, were used to determine the exact right and left ends. If necessary, integration sites were confirmed by the sequencing of PCR products encompassing the left or right boundary.

Measurement of GFP activity. To measure green fluorescent protein (GFP) activity, a microplate reader (model infinite M200; Tecan, Grodig, Austria) was used. Cells were grown in 150 μl of liquid culture in a 96-well plate (Greiner Bio-One, Frickenhausen, Germany; catalog number 655090) in a microplate reader at 30°C with occasional shaking. At 1-h intervals, cells were excited at 490 nm, and emission at 520 nm was measured. At the same time, the optical density (OD) of the cell culture was also measured at 600 nm at an optical-path length of 3.5 mm. To calculate GFP activity, the background emission was subtracted from the emission value, and the result was divided by the

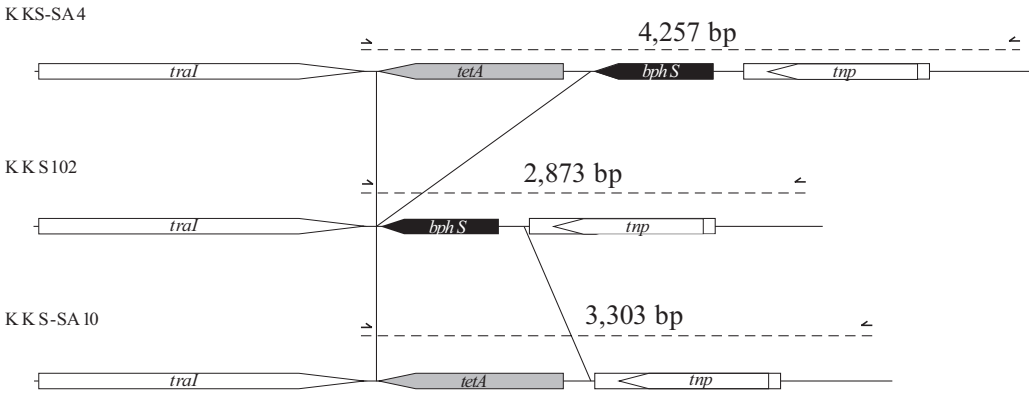

FIG 1 Schematic representation of the *bphS* regions of KKS102 (wild type), KKS-SA4, and KKS-SA10. KKS-SA4 carries the *tetA* gene from pBR322 downstream of *bphS*, and KKS-SA10 carries the *tetA* gene in place of *bphS*. See Materials and Methods for the construction of KKS-SA4 and KKS-SA10. The half-arrows indicate the primer-annealing sites of primer set 11 (Fig. 2 and 3), and the expected PCR product sizes are indicated above the dashed lines.

culture OD. To obtain the background emission value, cells with no *gfp* gene were grown, and a calibration curve for OD and background emission was made. This curve was used to calculate the background emission from the OD value.

Computer analysis. The search for tRNA genes was performed using tRNA finder at http://greengene.uml.edu/programs/FindtRNA.html (11). Comparative analysis was performed by creating a computational tool named CompareSequence, which is now part of the GenomeMatcher software (21) and is available at http://www.ige.tohoku.ac.jp/joho/gmProject/gmhome.html.

Nucleotide sequence accession number. The nucleotide sequence of ICE_{KKS102}*4677* was deposited in the DNA Data Bank of Japan under accession number AB546270.

RESULTS

Conjugal transfer of the *bph* locus from *Acidovorax* sp. KKS102 to proteobacterial strains. In designing our mating experiments, we decided to insert a tetracycline resistance marker into the *bph* locus and to select transconjugants by tetracycline resistance and not by the ability to utilize biphenyl as a sole carbon source. Because biphenyl and its degradation intermediates have an adverse effect on the cell viability of KKS102 (4), we speculated that selection in the presence of biphenyl might also inhibit the growth of the transconjugants. In addition, the full activation of the pE promoter, which directs transcription of the *bph* operon, requires a set of *bphPQ* genes (20). Because the *bphPQ* genes are thought to be distant from the *bph* operon and their orthologs are absent in UT26 and KT2440, the selection of transconjugants on biphenyl plates seemed inappropriate (after obtaining transconjugants, the transconjugants were tested for their ability to utilize biphenyl as a sole carbon and energy source, and we found that the transconjugants derived from ATCC 17616, but not those from UT26 and KT2440, could grow on biphenyl [data not shown]).

Two KKS102-derived strains, KKS-SA4 and KKS-SA10, were constructed to use as donors. KKS-SA4 carried a Tc^r gene 22 nucleotides downstream from *bphS* in the same direction, and KKS-SA10 carried the Tc^r gene in place of *bphS* (Fig. 1). The donor was mated with three recipient strains whose genome sequences have been determined: BmGm (a Gm-resistant derivative of *B. multivorans* ATCC 17616 [31, 37]), Sp-UTKm (a Km-resistant derivative of *Sphingobium japonicum* UT26 [15]), and Pp-KTGm (a Gm-resistant derivative of *P. putida* KT2440 [16]). ATCC 17616 carries a Tn*4371*-like element, but UT26 and KT2440 do not. Since our preliminary mating experiments using KKS-SA4 or KKS-SA10 as a donor suggested that in KKS-SA4 the circular-form ICE was increasingly formed toward the end of the exponential growth phase (data not shown), donor and recipient cells were grown to the exponential phase and then used.

In our initial mating experiment, the incubation period was 12 or 24 h, but we were unable to obtain transconjugants, and thus we extended the mating period to 4 days. After mating for 4 days, the cells were spread onto fresh medium containing an appropriate combination of antibiotics to select the Tc^r transconjugants. Colonies on the selection plates were tested for BphC activity (2,3-dihydroxybiphenyl *meta*-cleaving activity, which converts 2,3-dihydroxybiphenyl to a light-yellow compound), and BphC-positive clones from independent mating experiments were stored for further analyses. We could obtain transconjugants with these three recipient strains. For the BphC-negative clones, a PCR targeting the left part of the ICE (a DNA region spanning nucleotide positions 5531 to 6530) was conducted and no PCR products were observed, suggesting that these clones were spontaneous drug-resistant clones.

The frequencies of obtaining the transconjugants were very low. For example, in three independent mating experiments with KKS-SA4 and Pp-KTGm using 1.5×10^9 to 1.9×10^9 input donor cells, we obtained 0, 1, and 1 transconjugants after 4 days of incubation (the transfer frequency was 5.8×10^{-10} on average), while no transconjugants were obtained after 1, 2, and 3 days of mating. In addition, the number of transconjugants obtained by mating experiments using KKS-SA4 or KKS-SA10 as a donor was always low, regardless of the strain used as a recipient. We obtained only a few or no transconjugants in each mating experiment, and the transfer frequencies were on the order of 10^{-10} per donor.

By mating Pp-TKT1(a transconjugant obtained by mating Pp-KTGm and KKS-SA4) and PpY512 (a kanamycin-resistant derivative of *P. putida* PpY101), a BphC-positive and Tc-resistant clone was obtained. Because Pp-KTGm carried no related ICEs, the locus was indicated to be capable of autonomous transfer. Here, we refer to this mobile element as ICE_{KKS102}*4677*, according to the proposal for the nomenclature of mobile genetic elements (24).

Sequence determination of ICE_{KKS102}*4677*. To determine the complete nucleotide sequence of ICE_{KKS102}*4677*, a cosmid library of KKS102 (20) was searched by PCR for clones carrying either the

upstream or downstream region of the *bph* operon, resulting in two cosmid clones, pKH3000 and pKH5000, carrying downstream and upstream regions of the *bph* operon, respectively. These two cosmid clones were sequenced basically by primer walking. After an approximately 25-kb DNA region downstream of the *bph* operon was determined, several PCR primer sets that amplify different parts downstream from the *bph* operon were designed. These primer sets were used to investigate the presence of the corresponding DNA sequence in one of the transconjugants, Pp-TKT1, leading to the determination of the approximate right end of ICE$_{KKS102}$*4677*. Its precise right end in Pp-TKT1 was subsequently determined by DNA sequencing using its genomic DNA as a template (18) and a primer that annealed close to the approximate right end. The availability of the genome sequence of KT2440 allowed the identification of the exact right end. Based on the inference that ICE$_{KKS102}$*4677* was inserted at one site in the KT2440 genome, another primer was designed that anneals to a region beyond the insertion site, and the left junction of the mobile element in Pp-TKT1 was determined. The right and left terminal sequences of ICE$_{KKS102}$*4677* in Pp-TKT1 were both 5′-GATTTTAAG-3′.

The complete nucleotide sequence of the mobile element was 61,807 bp long (accession no. AB546270), and the nucleotide sequence was consistent with our recent determination of the whole genome sequence of KKS102 (our unpublished data).

ICE$_{KKS102}$*4677* in the KKS102 genome also had direct repeats of the 9-bp sequence at both ends, with the right end 190 bp from a cluster of three tRNA genes (tRNAGly, tRNACys, and tRNAGly) and the left end next to a gene for a conserved hypothetical protein. The integration sites of ICE$_{KKS102}$*4677* in the 13 transconjugants from independent mating experiments were determined by Sanger sequencing, in which total genomic DNA was used as a template (Table 2). In 8 out of 13 transconjugants from three different recipient strains, the sequence at both junctions between ICE$_{KKS102}$*4677* and the recipient genome was 5′-GATTTTAAG-3′, which precisely matched the end sequences of ICE$_{KKS102}$*4677*. This suggests that the recombination between the two 9-bp sequences, one on the circular form of ICE$_{KKS102}$*4677* (*attP*) and the other on the recipient genome (*attB*), resulted in the integration of ICE into the recipient genomes. It should be noted that the other 5 transconjugants had an integration of ICE$_{KKS102}$*4677* at a site that was not identical to 5′-GATTTTAAG-3′. It was deduced from the boundary sequences that the recombination occurred between nucleotide positions 7 and 8 or 8 and 9 of the 9-bp sequence (BmGmSA101 and BmGmSA103 in Table 2). These 5 transconjugants are all derived from *B. multivorans* ATCC 17616, and its genome carried eight copies of the sequence GATTTTAAG.

Organization of ICE$_{KKS102}$*4677*. The DNA sequence of ICE$_{KKS102}$*4677* was manually annotated with the aid of an annotation support tool (21) (Fig. 2). For simplicity, in this study, genes with an ambiguous function or that are apparently not related to conjugal transfer or PCB/biphenyl catabolism were designated open reading frames (ORFs) and serially numbered (see Table S2 in the supplemental material for the detailed annotation).

A gene for site-specific recombinase (*int*) belonging to the tyrosine recombinase family was found close to the left end of the ICE, and the *int* gene was oriented to the inward direction. The putative *xis* gene, whose product was 47% identical to the excisionase (RdfS) from the *Mesorhizobium loti* R7A-derived ICE for symbiosis (22), was located 20 kb from the *int* gene. The excisionase is an auxiliary and recombination directionality factor for the site-specific excision of mobile genetic elements.

Based on the comparative analysis of the related ICE-like elements (see below), four conserved gene blocks (the *int*, *parB*, *traI*, and *mpf* blocks) were identified. The regions flanked by these conserved gene blocks carry accessory genes. The region between the *int* and *parB* blocks harbors nine genes for hypothetical proteins. The region between the *parB* and *traI* blocks harbors eight genes that may be related to heavy metal resistance. The third region harbors genes for PCB/biphenyl catabolism. The last region harbors genes for a hypothetical protein, a DNA helicase, and a transposase. The presence of the accessory region next to *orf62* is rare but not specific to ICE$_{KKS102}$*4677*, and at least four related ICEs (ICEs 77, 90, 91, and 96 [see below]) carried an additional region.

Transconjugants carried the whole ICE$_{KKS102}$*4677*. In the previous work by Merlin et al., the right part of Tn*4371*, called Tn-*bph*, was shown to transfer conjugally between CH34 derivatives (12), but the exact boundaries of Tn-*bph* have not been determined, and it has been postulated that Tn-*bph* might be a recombinant between Tn*4371* and genes in CH34 (32). These previous findings raised concern about whether the transconjugants we obtained carried the whole ICE$_{KKS102}$*4677*. We therefore conducted a PCR-based analysis (Fig. 3) in which DNA regions overlapping each other were targeted for PCR amplification (Fig. 2 shows the PCR targets). As shown in Fig. 3, when the total DNAs of representative transconjugants were used, all PCRs except one amplified DNA fragments of the expected sizes. The only exception was the PCR target 19-2, which was probably due to the high GC content of the region and might not have been due to the absence of the region. In addition, DNA regions upstream and downstream of ICE$_{KKS102}$*4677* were not found in the transconjugants. These results clearly showed that the whole ICE, but not the ICE-flanking regions, was present in the transconjugants.

Identification and quantitation of circular-form ICE. To investigate whether ICE$_{KKS102}$*4677* is excised to generate its circular form in KKS102, a PCR primer set was designed that specifically detected the circular form (primers 1 and 2 in Fig. 4). PCR amplification yielded a band of the expected size, and the nucleotide sequence of the amplified product perfectly matched the expected sequence that was formed by the recombination between the GATTTTAAG sequences located at the extreme ends of ICE$_{KKS102}$*4677*. To investigate the ratio of KKS102 cells carrying the circular form to those carrying the integrated form, a quantitative PCR analysis was conducted. In this analysis, we used two sets of primers, one to detect the circular form and the other to detect both the circular and integrated forms. Four independent experiments, using a total DNA isolated from a KKS102 culture in its late log phase or early stationary phase, revealed that the circular form is present at frequencies ranging from 10^{-5} to 5×10^{-4}. Since ICEs are thought to form a circular intermediate before transfer to a recipient cell, this low rate might account for the ICE's low conjugal-transfer frequency.

To test whether the *int* gene is involved in the formation of the circular intermediate, a deletion mutant of the *int* gene (KKSA4Δint) was constructed. No circular-form DNA was detected by PCR using total DNA of the mutant as a template. The mutant complemented for the *int* gene using pReInt2 (a pNIT6012 derivative) restored the excision rate to a level comparable to that of the

TABLE 2 ICE integration sites

Transcongugant	Recipient	Replicon (chromosome)	Position		Integration target	Boundary		Integration site	Relative excision frequency[a]
			Start	End		Left	Right		
Pp-TKT1, Pp-KTGmSA151[b]	KTGm		4361712	4361720	GATTTTAAG	GATTTTAAG	GATTTTAAG	Intergenic region between PP3836 (hypothetical protein) and PP3837 (SURF4 domain protein)	0.15
BmGmSA33[b]	BmGm	I	1343869	1343877	GATGGTAAG	GATGGTAAG	GATTTTAAG	Within a gene encoding inactivated hemolysin activator	1.9
BmGmSA35[b]	BmGm	I	977691	977699	ATTCAGAAG	ATTCAGAAG	GATTTTAAG	Integenic region between BMULJ_00903 (copper resistance transmembrane protein) and BMULJ_00904 (response regulator for cupper resistance genes); within an accessory region of ICEATCC17616 (sequence 107)	0.02
BmGmSA101[b], BmGmSA103	BmGm	I	2631253	2361244	GATTTTGAG	GATTTTGAG	GATTTTAAG	tRNA-Leu gene	0.06
BmGmSA102[b]	BmGm	I	3445042	3445050	GACGGCAAG	GACGGCAAG	GATTTTAAG	Within a gene encoding a conserved hypothetical protein	0.6
BmKmSA36[b]	BmGm	III	434184	434192	GATTTTAAG	GATTTTAAG	GATTTTAAG	Within a gene encoding a truncated helicase	970
Sp-UTKmSA11, Sp-UTKmSA14, Sp-UTKmSA15, Sp-UTKmSA121[b], Sp-UTKmSA122	UTKm	I	2157304	2157312	GATTTTAAG	GATTTTAAG	GATTTTAAG	tRNA-Leu gene	81

[a] Excision frequency relative to that of KKS102.
[b] Strain used to investigate excision frequency.

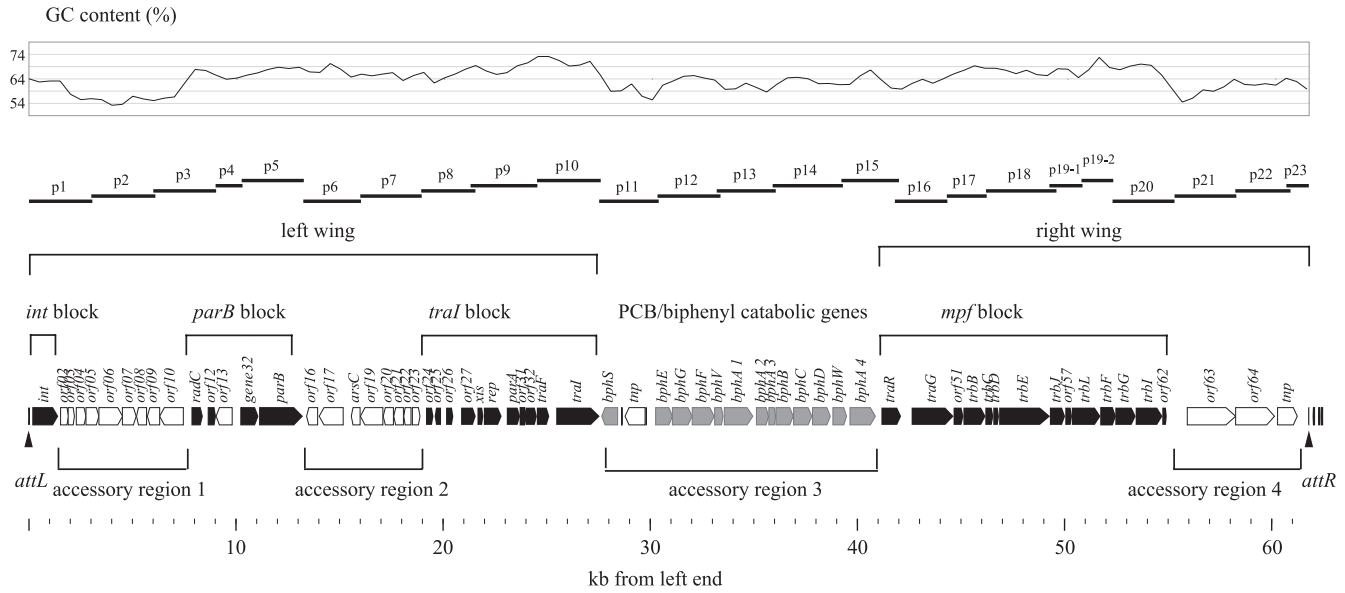

FIG 2 Structure of ICE$_{KKS102}$*4677*. Protein-coding genes found in ICE$_{KKS102}$*4677* are shown, along with position markers. The black arrows represent conserved genes, and the gray arrows represent PCB/biphenyl degradation genes. Four blocks of genes constituting the core structure of Tn*4371* family ICEs are indicated. The horizontal bars labeled p1 to p23 are the DNA regions targeted for PCR amplification in Fig. 3. The GC content is also shown.

wild-type strain (data not shown). These results indicate that the *int* gene has an essential role in the generation of the circular form.

High excision rate and high transposition frequency from BmGmSA36. The excision frequencies of ICE$_{KKS102}$*4677* in the transconjugants were also determined relative to that in KKS102. As shown in Table 2, each of the transconjugants exhibited a different excision frequency, and UTKmSA121 and BmKmSA36 exhibited much higher frequencies than the others. Because BmKmSA36 exhibited the highest excision frequency—3 orders of magnitude higher than that of KKS-SA4 (Table 2)—we expected that transconjugants would be obtained at a higher frequency by using BmKmSA36 as a donor. By an overnight mating of BmKmSA36 (donor) and Pp-KTGm (recipient), we obtained an average frequency of 1.2×10^{-7} in three independent experiments.

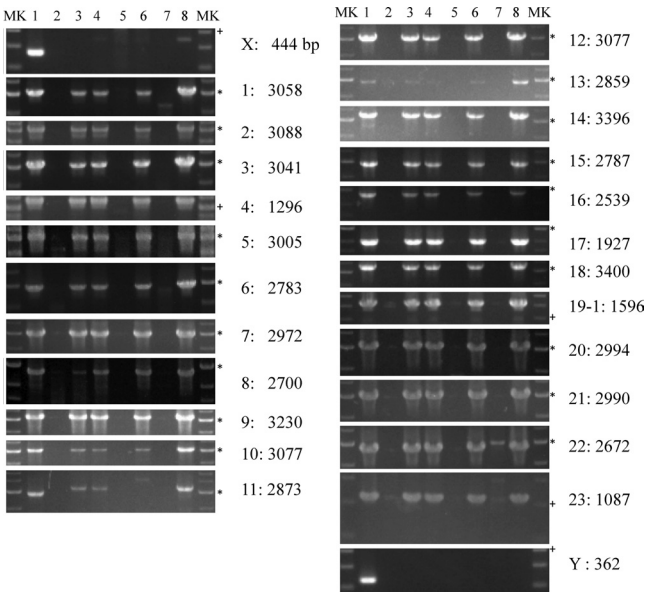

FIG 3 PCR-based detection of ICE subregions in transconjugants. Total DNA prepared from each strain was used as a template to test by PCR for the presence or absence of the ICE subregions. The lanes contain template DNA as follows: 1, KKS102; 2, BmGm; 3, BmGmSA33; 4, BmGmSA101; 5, Pp-KTGm; 6, Pp-TKT1; 7, Sp-UTKm; and 8, Sp-UTKmSA11. On the right of each gel are the names of the primer sets, as well as the expected PCR sizes in base pairs. The 3-kb (*) and 1-kb (+) bands are marked. Figure 2 shows the amplification target of each primer set, and Fig. 1 shows the interpretations of the results for primer set 11. Primer sets X and Y target DNA regions upstream and downstream of ICE$_{KKS102}$*4677*, respectively.

Promoter activities of *int* in the integrated and circular forms. The integrase gene (*int*) in *P. knackmussii* B13 is located at the end of the ICE in the inward direction and is transcribed from an external promoter in the integrated form, whereas in the circular form, it is transcribed from a promoter located on the other end of the same ICE. The *int* gene of B13 is highly transcribed when the ICE is in its circular form (29). To test whether the *int* gene in KKS102 is transcribed in a similar manner, the promoter activities of upstream DNA regions of *int* in the circular and integrated forms (Fig. 4A shows the details) were measured. Each promoter was placed in front of *gfp-lacZ* reporter genes on pKLZG and integrated into a selected genomic locus by homologous recombination (see reference 30 for details). As expected, the activity of the integrase promoter of the circular form was significantly higher than that in the integrated form (Fig. 5), which was close to the detection limit of GFP activity measurement. Therefore, the ICE$_{KKS102}$*4677* integrase gene was highly transcribed in its circular form. This feature of ICE integrase might help the circular entity to be promptly integrated into the genome after entering the recipient cell. To test the possible circuits of transcriptional regulation of the *int* gene, its promoter activity was also analyzed in the *bphS* and *traR* mutants (Fig. 5). We included *traR*, which encodes a LysR-type transcriptional regulator (*traR* was originally called *bphR*; the name was changed because of its conservation among

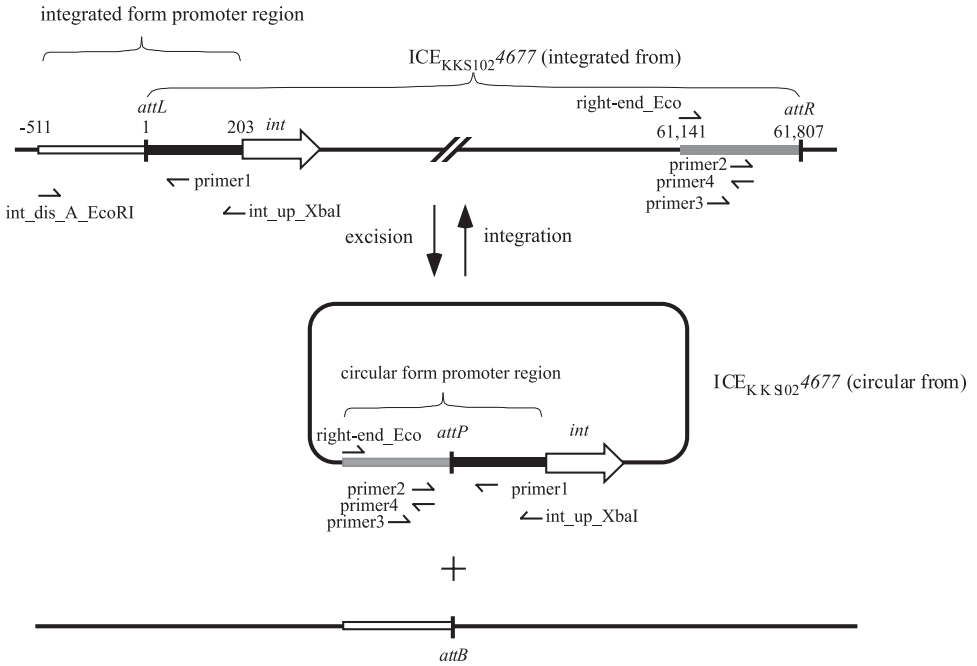

FIG 4 Schematic representation of the circular and integrated forms of ICE$_{KKS102}$*4677*. The integrated form of ICE generates, by excision, a circular form of ICE and a genomic locus devoid of ICE. Two primer sets were designed to detect the circular form (primers 1 and 2) and both of the forms (primers 3 and 4). The promoter regions fused with *gfp-lacZ* to analyze *int* promoter activity are also shown, and the primers used to amplify these regions are indicated: int_dis-_A_EcoRI and int_up_XbaI for the integrated-form promoter, and right-end_Eco and int_up_XbaI for the circular-form promoter. The numbers indicate the nucleotide positions relative to the left end of ICE$_{KKS102}$*4677*.

ICEs). As the *traR* promoter is negatively regulated by BphS (our unpublished observation), a cascade of regulation that senses the presence of a pathway substrate and enhances the conjugation frequency was expected. Contrary to our expectation, the *int* promoter activities of both forms were unaffected in the two mutants. Because the GFP activities of the integrated-form promoter were low, we also measured the promoter activity by LacZ, which allows more sensitive measurement, but the activities

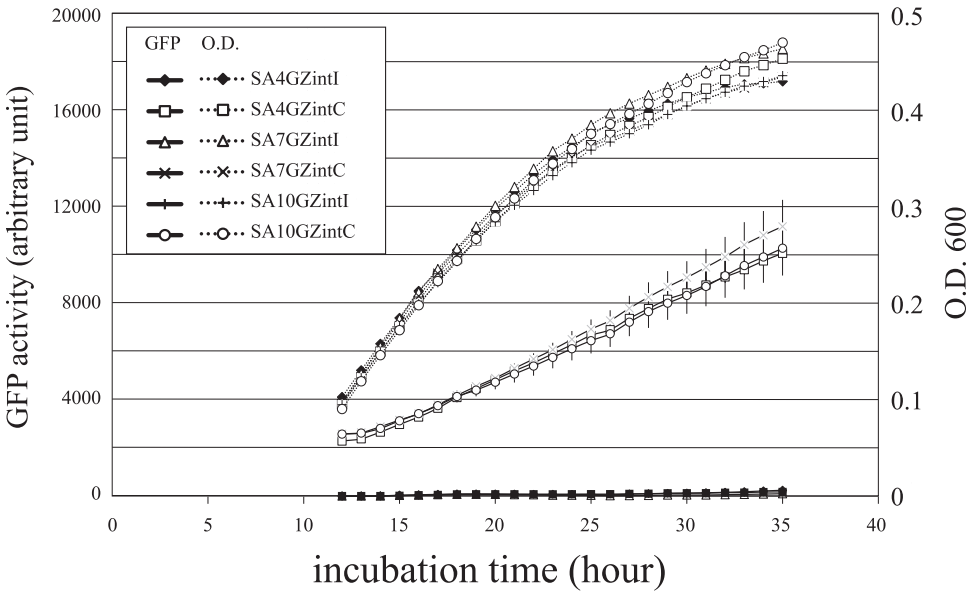

FIG 5 *int* gene promoter activities in its circular and integrated forms. Circular-form *int* promoter activities were measured in the wild-type (SA4GZintC), *bphS*-mutated (SA10GZintC), and *traR*-mutated (SA7GZintC) strains. Integrated-form *int* promoter activities were measured in the wild-type (SA4GZintI), *bphS*-mutated (SA10GZintI), and *traR*-mutated (SA7GZintI) strains. Four independent experiments were carried out for each strain, and standard deviations are shown for the GFP activities of strains carrying the circular form of ICE$_{KKS102}$*4677*. As the GFP activity at low OD is less reliable, the GFP activities obtained with an OD value of 0.1 are shown.

were not affected in the two mutants (data not shown). The quantification of the excised form in both mutants suggested that the excision is not under the control of these regulatory genes (data not shown).

Comparative analysis of related ICEs to establish the border of the Tn*4371* family of ICEs. Tn*4371*-related ICE-like elements from beta- and gammaproteobacteria have been well documented in recent articles. Ryan et al. described 18 Tn*4371*-related ICEs (27), and Van Houdt et al. recently described Tn*4371*-related ICEs found in beta- and gammaproteobacteria (34), as well as one from alphaproteobacteria. These two articles well described the conserved genes among these ICEs. However, a search of the public database using a TraG amino acid sequence identified many other TraG-encoding DNA sequences that also encoded other homologous genes found on ICE$_{KKS102}$Tn*4677*. To establish an ICE family, it is important to collect as many similar elements as possible and then analyze them with respect to gene contents and gene organization. If a group of ICE-like elements that share genetic traits is found, and the elements belonging to the group are distinct from the other elements, such a group is considered an ICE family.

To this end, the public database was searched by using the TraG amino acid sequence from ICE$_{KKS102}$*4677* as a query, and a total of 112 TraG homologues were collected (see Table S3 in the supplemental material) and used for a phylogenetic analysis. (Although we also searched the database by using the TraI amino acid sequence as a query, we found no additional DNA sequences that carried a similar full-length ICE-like element.) As shown in Fig. 6, the TraG amino acid sequences could be classified into four groups. One group (designated a plasmid cluster: sequences 1 to 13 in Fig. 6) contained TraG sequences from plasmids, including the RP4 plasmid, that are relatively small, around 80 kb and 224 kb at most. Investigation of these *traG*-encoding plasmids revealed that the content and order of genes relevant to horizontal transfer were distinct from those of ICE$_{KKS102}$*4677*. Two groups, designated α clusters I (αI; sequences 20 to 65) and II (αII; 66 to 74), consisted of TraG sequences exclusively from alphaproteobacteria. The last group (the βγ group) included TraG from beta- and gammaproteobacteria (sequences 75 to 112) but no TraG from alphaproteobacteria. The genomes encoding TraG homologues that belong to the last three groups were searched for ICE-like elements by using the computational tool GenomeMatcher (21), as well as a computational tool named CompareSequences that we developed for this purpose and that is now available as one of the accessory tools of GenomeMatcher. Here, we refer to ICE-like elements encoding a TraG homologue belonging to the αI, αII, and βγ groups as αI-type ICEs, αII-type ICEs, and βγ-type ICEs, respectively. We found 35 αI-type, 8 αII-type, and 31 βγ-type ICEs.

Table S4 in the supplemental material shows the locations, as well as the terminal direct repeats, of the βγ-type ICEs. For each βγ-type ICE, when a gene conserved among the Tn*4371* family ICEs was not being annotated, the gene was searched, and we found 12 genes (see Table S5 in the supplemental material); for example, a *radC* homologue in *Pseudomonas aeruginosa* PA7 was found (sequence 96). All of the ICE-like elements were analyzed with respect to the presence of the reported conserved genes among Tn*4371*-like ICEs, as well as with respect to the order of genes within conserved gene blocks. The gene conservation as expressed by sequence identities at the amino acid level is shown in Table S5 in the supplemental material, while Fig. S1 shows the gene organization of the βγ-type and Fig. S2 shows that of the αI- and αII-type ICEs. These data clearly showed that βγ-type ICEs are distinguishable from αI- and αII-type ICEs (see Discussion for details).

***att* sites.** The direct repeat of ICE$_{KKS102}$*4677* (GATTTTAAG) is different from that of Tn*4371* (TTTTTCAT) and those of the related ICEs reported by Ryan et al. (TTTTT/CA/GT). We attempted to identify the right- and left-end sequences of the newly identified Tn*4371*-related elements in beta- and gammaproteobacteria, as well as those missing in the report by Ryan et al. The presumed left- and right-end sequences are shown, along with the neighbor-joining tree of the Int proteins, in Fig. S3 in the supplemental material. There seems to be a strong correlation between the amino acid sequences of Int proteins and the nucleotide sequences of the *att* sites, i.e., the Int proteins that were similar to each other seemed to recognize similar *att* sites. Of note, ICEs from KKS102 (number 102), *Thioalkalivibrio* sp. strain HL-EbGR7 (number 99), and *P. aeruginosa* UCBPP PA14 (number 98) were flanked by the same 9-bp repeat, GATTTT AAG. In addition, there seemed to be a group of Int proteins that recognizes *att* sites of A/TTTTTGAG (numbers 77, 100, and 101). Therefore, the *att* sites of the Tn*4371* family ICE are not limited to TTTTT/CA/GT.

DISCUSSION

PCB/biphenyl degradation genes are located on ICEs. In this study, several lines of evidence demonstrated that a PCB/biphenyl degradation locus in KKS102 was part of an ICE. First, covalently bound left and right sequences were detected by PCR, which indicated the presence of an excised circular form. The presence of the circular form was dependent on the intact *int* gene located at the extreme left. Second, by performing mating experiments with different proteobacterial strains, we obtained transconjugants and identified the genomic location at which the ICE was integrated. Third, although further functional characterization is needed, genes that might play roles at various stages of transposition from the host genome to the recipient genome were identified on the ICE. They include genes for excision of ICE (integrase and excisionase), nicking at *oriT* and unwinding (relaxase), DNA transfer machinery (transfer of single-stranded DNA molecules), and the formation of double-stranded circular molecules (cyclase). Fourth, KKS102 carries no plasmids, and the *bph* locus was located on the KKS102 chromosome (data not shown). Following the suggestions for the nomenclature of the mobile genetic element (24), we named this mobile genetic element ICE$_{KKS102}$*4677*.

Transfer frequency of ICE$_{KKS102}$*4677*. The frequency of transfer of ICE$_{KKS102}$*4677* from KKS-SA4 to the recipients tested was low, and a long mating period was required to obtain transconjugants. This could have been due to the low level of the excision of ICE$_{KKS102}$*4677* in KKS-SA4. Although the possibility that a Tn*4371*-like element residing in ATCC 17616 (the parental strain of BmKmSA36) enhanced the frequency could not be excluded, when BmKmSA36, in which the excised form was detected at a higher rate, was used as a donor, we could obtain transconjugants at a much higher transfer frequency by overnight mating.

The high excision frequency in BmKmSA36 might have been due to the presence of a promoter located close to the integration site that directed the transcription of the *int* gene of ICE$_{KKS102}$*4677*. In this sense, the excision and possibly the transfer

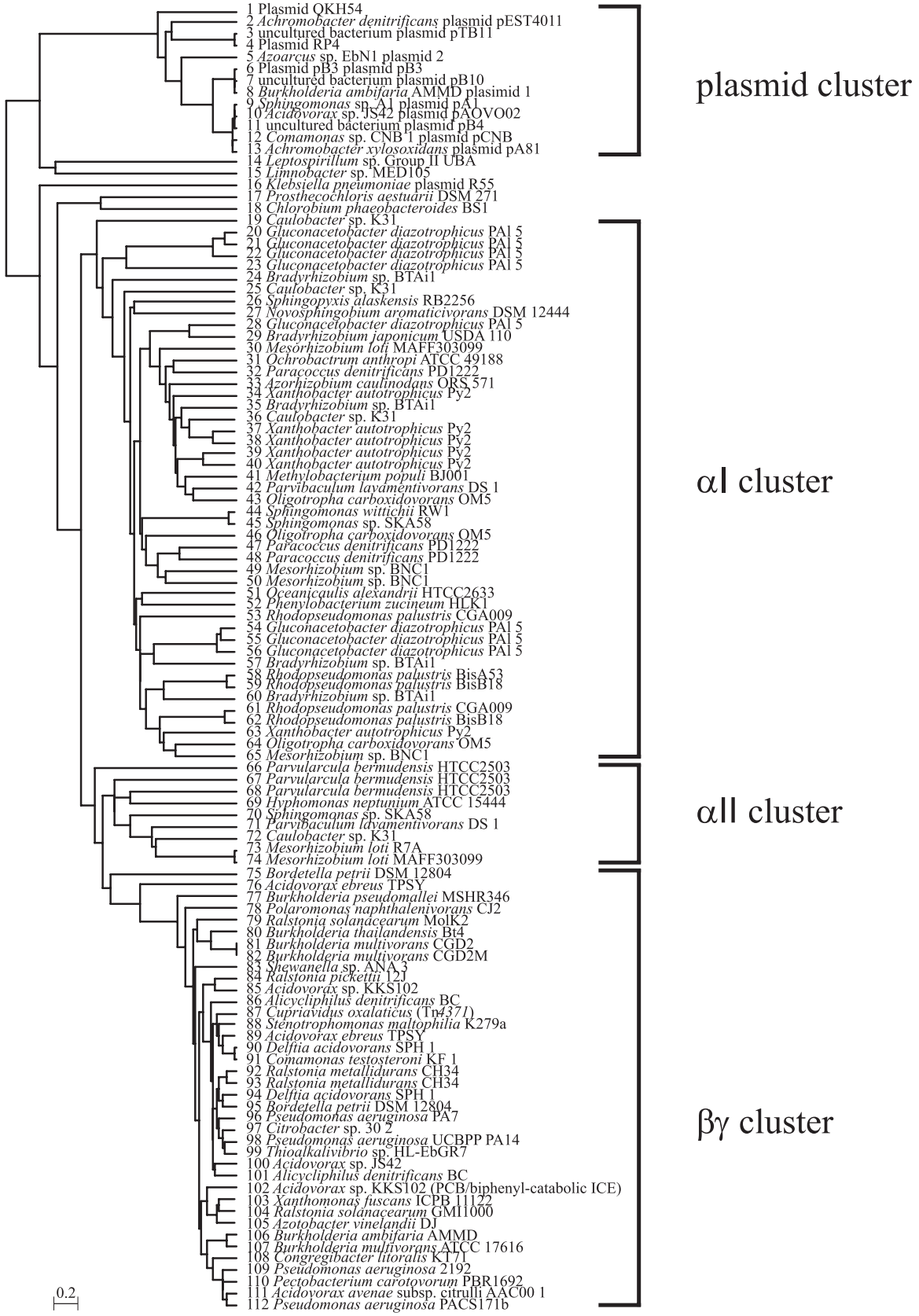

FIG 6 Phylogenetic analysis of TraG amino acid sequences. The amino acid sequences were aligned by MAFFT version 6 (7), and a phylogenetic tree was drawn by using the unweighted-pair group method using average linkages (UPMGA). TraG amino acid sequences were retrieved by a BLASTP search against the nr database at the NCBI website in October 2008, and for the β and γ clades, an additional search was performed in August 2010. See Table S2 in the supplemental material for the accession numbers of the TraG sequences and the sizes of the replicons that encode the TraG homologue. The numbers 87 and 102 represent Tn*4371* and ICE_{KKS102}*4677*, respectively.

of an ICE that carries the inwardly oriented *int* gene might be strongly affected by the presence of a promoter that is located close to the integration site and directs the transcription of the *int* gene.

Phylogeny of TraG. The shape of the phylogenetic tree suggests interesting issues regarding the evolution of KKS102-type ICEs. It seems that from a prototypical ICE present only in alphaproteobacteria an ICE emerged that gained the ability to prevail in beta-and gammaproteobacteria but at the same time lost the ability to disseminate in alphaproteobacteria. The branches in the β and γ clades are shorter than those in the α clade, suggesting that this gain and loss of ability was accompanied by an increase in the transpositional activity. The short branch length was also consistent with the conservation of gene content and order among Tn*4371* family ICEs. This is in marked contrast to the situation in α clusters I and II, where putative ICEs are so highly diverged in gene content and gene organization that it seems difficult to define α-type ICEs.

Discrimination of Tn*4371* family ICEs from other ICE-like elements. We conducted comprehensive analysis of the three types of putative ICEs (αI-type, αII-type, and βγ-type ICEs) with respect to gene content and gene organization. We showed that the gene content and gene organization of βγ-type ICEs are clearly distinguishable from those of the αI-type and αII-type ICEs. In βγ-type ICEs, the conserved genes were found to constitute four blocks (see Fig. S1 in the supplemental material for details): (i) the *int* gene block, containing only the *int* gene; (ii) the *parB* block, containing four conserved genes (*radC*, *orf12*, *gene32*, and *parB*); (iii) the *traI* block, containing 11 conserved genes; and (iv) the *mpf* block, containing genes for mating-pair formation, including the *traG* gene. Although some genes were not found in a minor fraction of the ICEs, the order of the four gene blocks was invariable, as was the order of genes within each block (see Fig. S1 in the supplemental material).

The analysis of Tn*4371*-like elements of the αI- and αII type ICEs showed that these elements were different from those of the βγ-type ICEs with respect to the gene content and organization. None of them did not carry the complete set of genes in the *parB* block, and most of them lacked a gene similar to *orf25* in KKS102. The *traR* gene homologues were often found at different locations, and the *traG* gene was often separated from the rest of the genes for mating-pair formation. Often, no genes were found between the *traI* and *traG* genes, which corresponded to accessory region 3 of the βγ-type ICEs. The *int* gene was missing in half of the elements. These significant differences indicated that these αI-, αII-, and βγ-type ICEs should not be included within a single family of ICEs.

Based on the DNA sequence analysis and its intracellular transposition, Tn*4371* (sequence 87) has been considered an ICE, but its intercellular transfer has not yet been demonstrated (27, 32). In this paper, we demonstrated the horizontal transfer of ICE$_{KKS102}$*4677* for the first time as a member of this type of ICE from a donor chromosome to a recipient chromosome.

We noticed that in some cases *int* genes with no detectable sequence similarity or with low sequence similarity to that in KKS102 were present at the extreme left of this type of ICE (numbers 75, 76, 79, 92, and 107) (see Fig. S3 in the supplemental material). This could be due to the nature of ICEs, which are made up of interchangeable functional modules (35). Therefore, defining this type of ICE by the presence of a similar integrase gene (27) seems to be inappropriate.

Comparison of ICE$_{KKS102}$*4677* with other ICEs. To better understand the Tn*4371* family ICEs, ICE$_{KKS102}$*4677* was compared with ICEs belonging to different families with respect to the gene content and organization. Compared with the *clc* element from *P. knackmussii* B13, among the ICE backbone genes of ICE$_{KKS102}$*4677*, *radC*, *parA*, and *int* showed weak similarity at the amino acid level (48%, 26%, and 21%, respectively), while some metabolic gene products for PCB/biphenyl on ICE$_{KKS102}$*4677* showed certain levels of amino acid sequence similarity to those for chlorobenzoate on the *clc* element (BphE [55%], BphG [83%], BphF [86%], and BphA1 [28%]). With conjugative genomic island R391 (1), only two genes were conserved and showed 19% (Int) and 54% (RadC) identity at the amino acid level. With ICE*Ec2* from *E. coli* strain BEN374 (belonging to the pKLC102/PAGI-2 family) (26), only *int* was conserved and showed 28% identity at the amino acid level. No sequence similarity, even at the amino acid level, was found for Tn*916* from *Enterococcus faecalis* DS16 (25). Therefore, the gene content and organization of Tn*4371* family ICEs are distinct from those of different ICE families.

ACKNOWLEDGMENT

This work was supported by a Grant-in-Aid from the Ministry of Education, Culture, Sports, Science, and Technology of Japan.

REFERENCES

1. **Boltner D, MacMahon C, Pembroke JT, Strike P, Osborn AM.** 2002. R391: a conjugative integrating mosaic comprised of phage, plasmid, and transposon elements. J. Bacteriol. **184**:5158–5169.
2. **Burrus V, Pavlovic G, Decaris B, Guedon G.** 2002. Conjugative transposons: the tip of the iceberg. Mol. Microbiol. **46**:601–610.
3. **Burrus V, Waldor MK.** 2004. Shaping bacterial genomes with integrative and conjugative elements. Res. Microbiol. **155**:376–386.
4. **Delawary M, Ohtsubo Y, Ohta A.** 2003. The dual functions of biphenyl-degrading ability of Pseudomonas sp. KKS102: energy acquisition and substrate detoxification. Biosci. Biotechnol. Biochem. **67**:1970–1975.
5. **Dennis JJ, Zylstra GJ.** 1998. Plasposons: modular self-cloning minitransposon derivatives for rapid genetic analysis of gram-negative bacterial genomes. Appl. Environ. Microbiol. **64**:2710–2715.
6. **Fukuda M, et al.** 1994. Identification of the *bphA* and *bphB* genes of *Pseudomonas* sp. strains KKS102 involved in degradation of biphenyl and polychlorinated biphenyls. Biochem. Biophys. Res. Commun. **202**:850–856.
7. **Katoh K, Misawa K, Kuma K, Miyata T.** 2002. MAFFT: a novel method for rapid multiple sequence alignment based on fast Fourier transform. Nucleic Acids Res. **30**:3059–3066.
8. **Kikuchi Y, et al.** 1994. Identification of the *bphA4* gene encoding ferredoxin reductase involved in biphenyl and polychlorinated biphenyl degradation in *Pseudomonas* sp. strain KKS102. J. Bacteriol. **176**:1689–1694.
9. **Kikuchi Y, Yasukochi Y, Nagata Y, Fukuda M, Takagi M.** 1994. Nucleotide sequence and functional analysis of the meta-cleavage pathway involved in biphenyl and polychlorinated biphenyl degradation in *Pseudomonas* sp. strain KKS102. J. Bacteriol. **176**:4269–4276.
10. **Kimbara K, et al.** 1989. Cloning and sequencing of two tandem genes involved in degradation of 2,3-dihydroxybiphenyl to benzoic acid in the polychlorinated biphenyl-degrading soil bacterium *Pseudomonas* sp. strain KKS102. J. Bacteriol. **171**:2740–2747.
11. **Lowe TM, Eddy SR.** 1997. tRNAscan-SE: a program for improved detection of transfer RNA genes in genomic sequence. Nucleic Acids Res. **25**: 955–964.
12. **Merlin C, Springael D, Toussaint A.** 1999. Tn*4371*: a modular structure encoding a phage-like integrase, a *Pseudomonas*-like catabolic pathway, and RP4/Ti-like transfer functions. Plasmid **41**:40–54.
13. **Miller WG, Lindow SE.** 1997. An improved GFP cloning cassette designed for prokaryotic transcriptional fusions. Gene **191**:149–153.

14. **Miyazaki R, Ohtsubo Y, Nagata Y, Tsuda M.** 2008. Characterization of the traD operon of naphthalene-catabolic plasmid NAH7: a host-range modifier in conjugative transfer. J. Bacteriol. **190**:6281–6289.
15. **Nagata Y, et al.** 2010. Complete genome sequence of the representative γ-hexachlorocyclohexane-degrading bacterium *Sphingobium japonicum* UT26. J. Bacteriol. **192**:5852–5853.
16. **Nelson KE, et al.** 2002. Complete genome sequence and comparative analysis of the metabolically versatile *Pseudomonas putida* KT2440. Environ. Microbiol. **4**:799–808.
17. **Nishi A, Tominaga K, Furukawa K.** 2000. A 90-kilobase conjugative chromosomal element coding for biphenyl and salicylate catabolism in *Pseudomonas putida* KF715. J. Bacteriol. **182**:1949–1955.
18. **Nishiyama E, Ohtsubo Y, Nagata Y, Tsuda M.** 2010. Identification of *Burkholderia multivorans* ATCC 17616 genes induced in soil environment by in vivo expression technology. Environ. Microbiol. **12**:2539–2558.
19. **Ohtsubo Y, et al.** 2001. BphS, a key transcriptional regulator of *bph* genes involved in polychlorinated biphenyl/biphenyl degradation in *Pseudomonas* sp. KKS102. J. Biol. Chem. **276**:36146–36154.
20. **Ohtsubo Y, Goto H, Nagata Y, Kudo T, Tsuda M.** 2006. Identification of a response regulator gene for catabolite control from a PCB-degrading beta-proteobacteria, Acidovorax sp. KKS102. Mol. Microbiol. **60**:1563–1575.
21. **Ohtsubo Y, Ikeda-Ohtsubo W, Nagata Y, Tsuda M.** 2008. GenomeMatcher: a graphical user interface for DNA sequence comparison. BMC Bioinformatics **9**:376.
22. **Ramsay JP, Sullivan JT, Stuart GS, Lamont IL, Ronson CW.** 2006. Excision and transfer of the *Mesorhizobium loti* R7A symbiosis island requires an integrase IntS, a novel recombination directionality factor RdfS, and a putative relaxase RlxS. Mol. Microbiol. **62**:723–734.
23. **Ravatn R, Studer S, Springael D, Zehnder AJ, van der Meer JR.** 1998. Chromosomal integration, tandem amplification, and deamplification in *Pseudomonas putida* F1 of a 105-kilobase genetic element containing the chlorocatechol degradative genes from *Pseudomonas* sp. strain B13. J. Bacteriol. **180**:4360–4369.
24. **Roberts AP, et al.** 2008. Revised nomenclature for transposable genetic elements. Plasmid **60**:167–173.
25. **Roberts AP, Mullany P.** 2009. A modular master on the move: the Tn*916* family of mobile genetic elements. Trends Microbiol. **17**:251–258.
26. **Roche D, et al.** 2010. ICE*Ec2*, a new integrative and conjugative element belonging to the pKLC102/PAGI-2 family, identified in *Escherichia coli* strain BEN374. J. Bacteriol. **192**:5026–5036.
27. **Ryan MP, Pembroke JT, Adley CC.** 2009. Novel Tn*4371*-ICE like element in *Ralstonia pickettii* and genome mining for comparative elements. BMC Microbiol. **9**:242.
28. **Sambrook J, Fritsch EF, Maniatis T.** 1989. Molecular cloning: a laboratory manual, 2nd ed. Cold Spring Harbor Laboratory Press, Cold Spring Harbor, NY.
29. **Sentchilo V, Zehnder AJ, van der Meer JR.** 2003. Characterization of two alternative promoters for integrase expression in the *clc* genomic island of *Pseudomonas* sp. strain B13. Mol. Microbiol. **49**:93–104.
30. **Sota M, et al.** 2006. Functional analysis of unique class II insertion sequence IS*1071*. Appl. Environ. Microbiol. **72**:291–297.
31. **Stanier RY, Palleroni NJ, Doudoroff M.** 1966. The aerobic pseudomonads: a taxanomic study. J. Gen. Microbiol. **43**:159.
32. **Toussaint A, et al.** 2003. The biphenyl- and 4-chlorobiphenyl-catabolic transposon Tn*4371*, a member of a new family of genomic islands related to IncP and Ti plasmids. Appl. Environ. Microbiol. **69**:4837–4845.
33. **Van Houdt R, Monchy S, Leys N, Mergeay M.** 2009. New mobile genetic elements in Cupriavidus metallidurans CH34, their possible roles and occurrence in other bacteria. Antonie Van Leeuwenhoek **96**:205–226.
34. **Van Houdt R, et al.** 2012. The Tn*4371* ICE family of bacterial mobile genetic elements. *In* Roberts AP, Mullany P (ed), Bacterial integrative mobile genetic elements. Landes Bioscience, Austin, TX. http://www.landesbioscience.com/curie/chapter/5251/.
35. **Wozniak RA, Waldor MK.** 2010. Integrative and conjugative elements: mosaic mobile genetic elements enabling dynamic lateral gene flow. Nat. Rev. Microbiol. **8**:552–563.
36. **Yanisch-Perron C, Vieira J, Messing J.** 1985. Improved M13 phage cloning vectors and host strains: nucleotide sequences of the M13mp18 and pUC19 vectors. Gene **33**:103–119.
37. **Yuhara S, et al.** 2008. Pleiotropic roles of iron-responsive transcriptional regulator Fur in *Burkholderia multivorans*. Microbiology **154**:1763–1774.